Supporting Information for "Tuning the ORR activity of Pt-based Ti_2CO_2 MXene by varying the atomic cluster size and doping foreign metals"

Xilin Zhang,[a] Yiying Zhang,[a] Cheng Cheng,[b] Zongxian Yang *[ac] and Kersti Hermansson [d]

[a] School of Physics, Henan Normal University, *Henan Key Laboratory of Photovoltaic Materials,* Xinxiang 453007, China.

[b] College of Chemistry, Key Laboratory of Theoretical & Computational Photochemistry of Ministry of Education, Beijing Normal University, Beijing 100875, China

[c] National Demonstration Center for Experimental Physics Education (Henan Normal University), Xinxiang, 453007, China

[d] Department of Chemistry—Ångström Laboratory Uppsala University, Box 538, S-75121 Uppsala, Sweden

*Corresponding authors: yzx@henannu.edu.cn; kersti.hermansson@kemi.uu.se

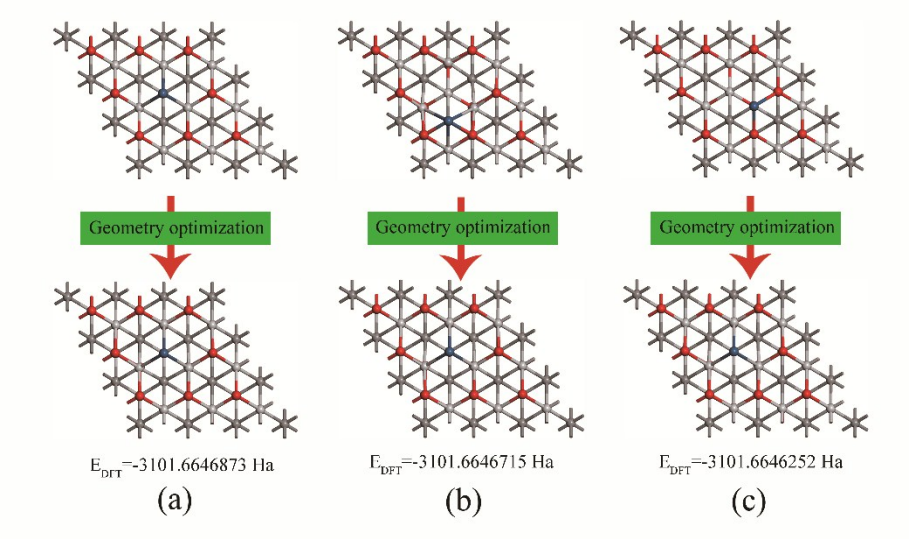

Fig. S1. The possible configurations of Pt/v-Ti_2CO_2 before and after geometry optimization.

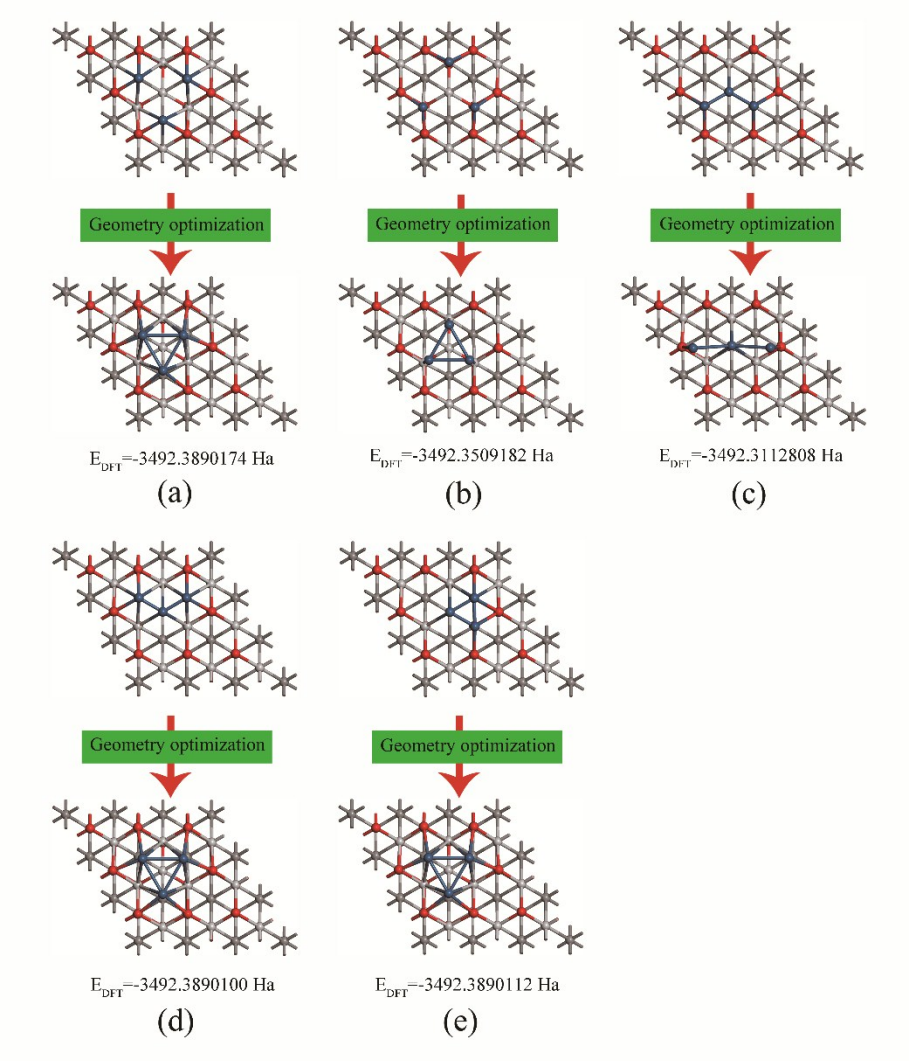

Fig. S2. The possible configurations of Pt_3/v-Ti_2CO_2 before and after geometry optimization.

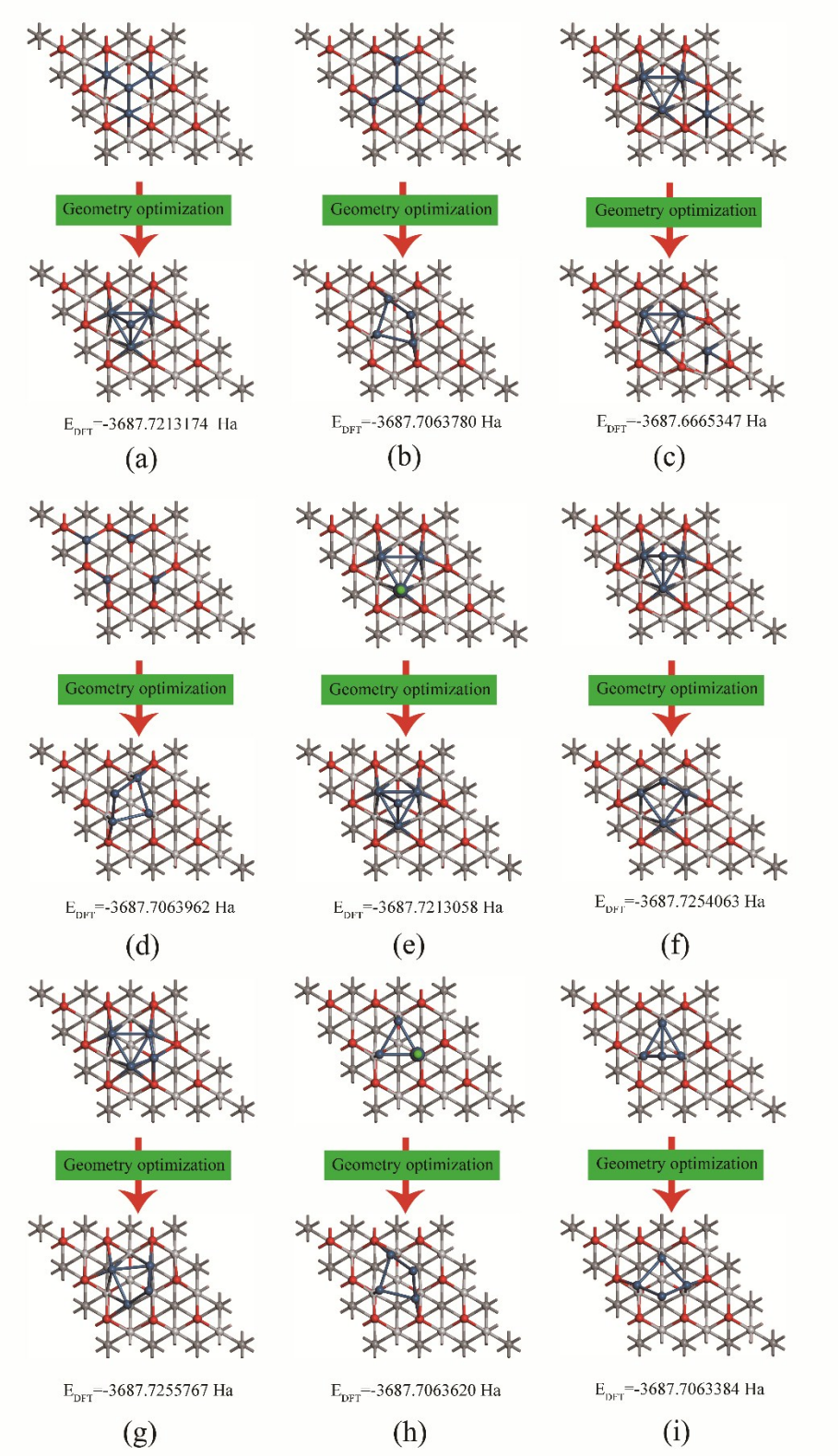

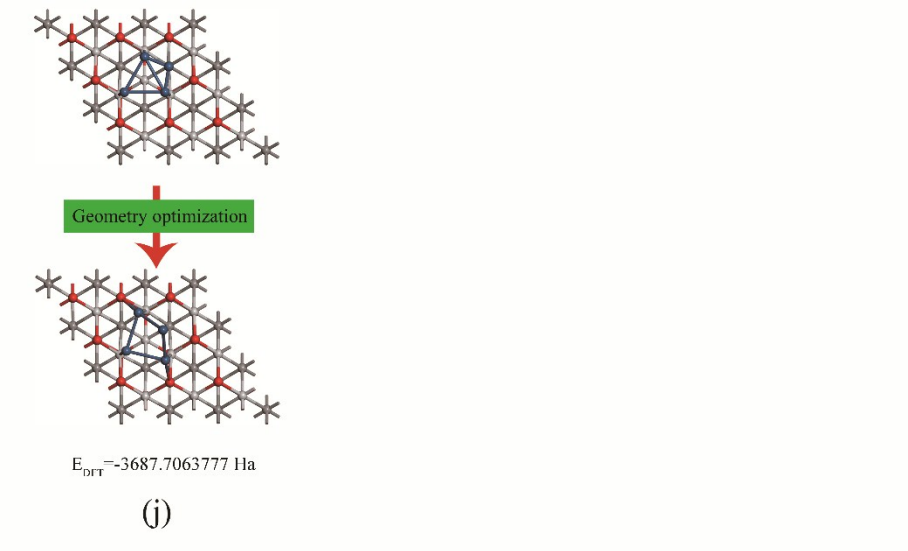

Fig. S3. The possible configurations of Pt_4/v-Ti_2CO_2 before and after geometry optimization. The bigger atoms displayed in the models denotes the bottom atoms of the overlapped atoms. The green ball represents the atomic Pt when two Pt atoms overlap.

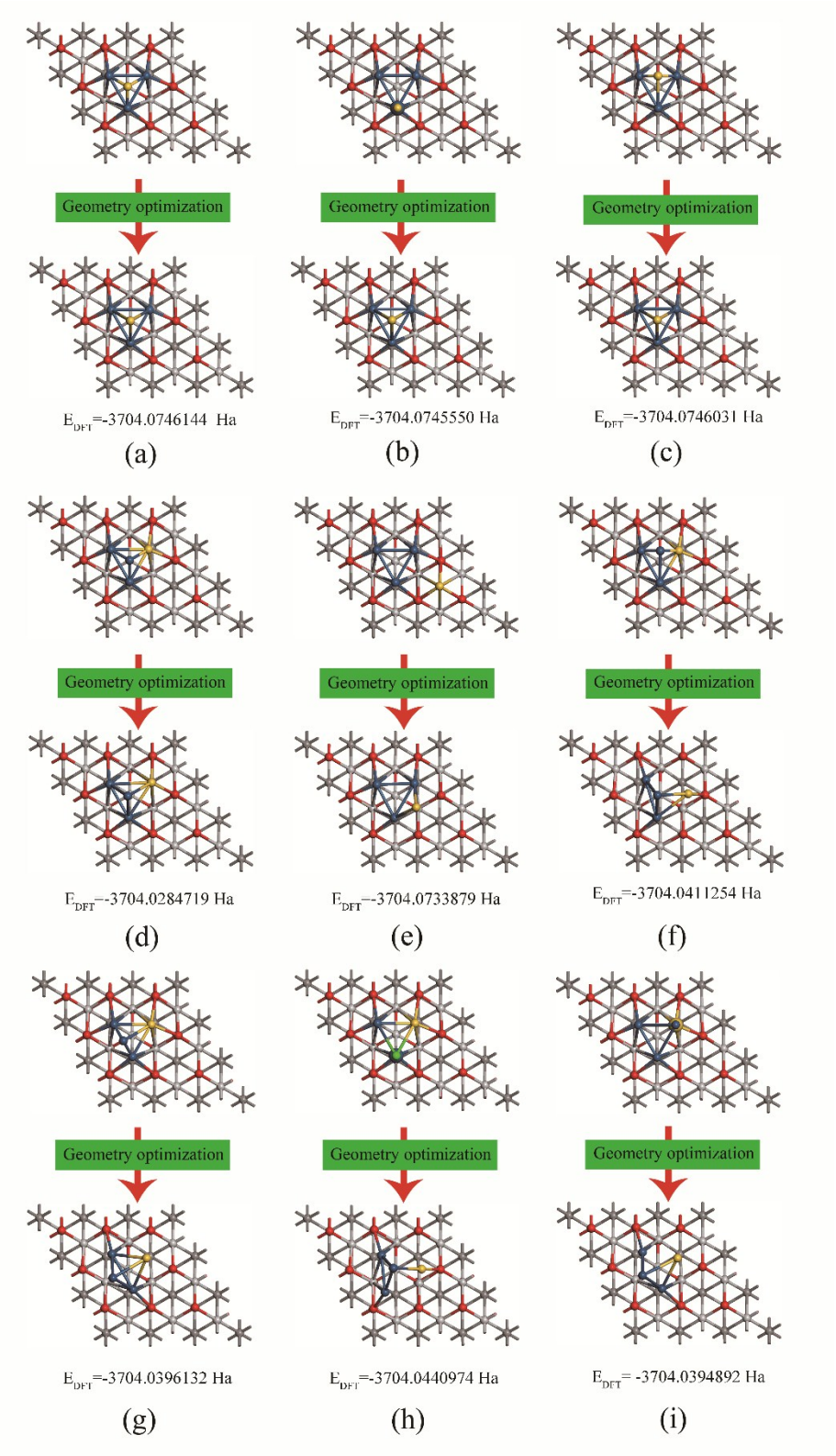

Fig. S4. The possible configurations of $Pt_3Au/v\text{-}Ti_2CO_2$ before and after geometry optimization.

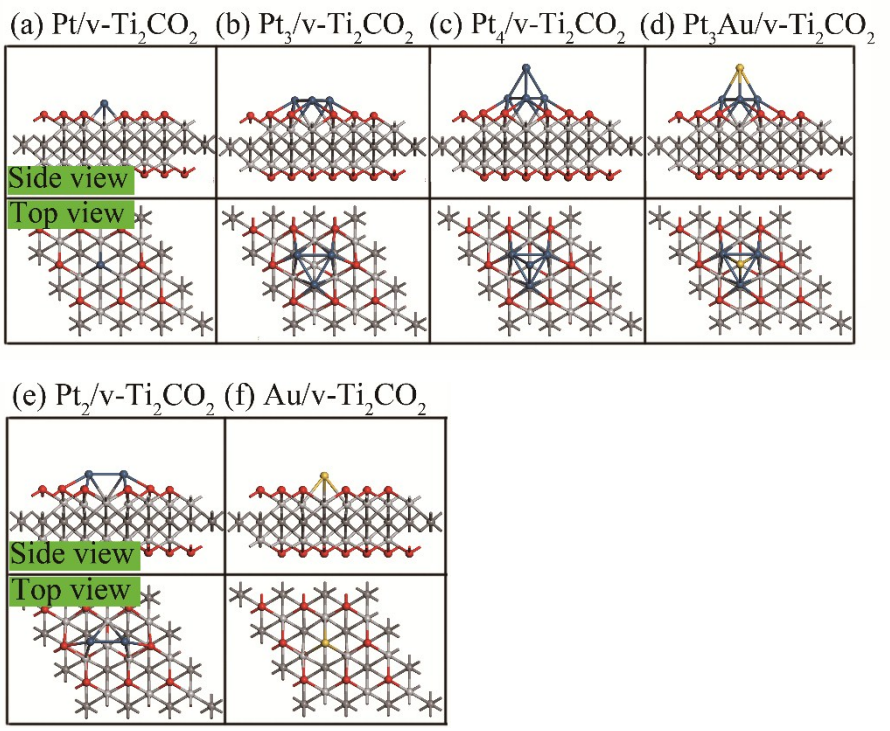

Fig. S5. Top and side views of the optimized geometric configurations of $Pt/v\text{-}Ti_2CO_2$, $Pt_2/v\text{-}Ti_2CO_2$, $Pt_3/v\text{-}Ti_2CO_2$, $Pt_4/v\text{-}Ti_2CO_2$, $Pt_3Au/v\text{-}Ti_2CO_2$ and $Au/v\text{-}Ti_2CO_2$ systems.

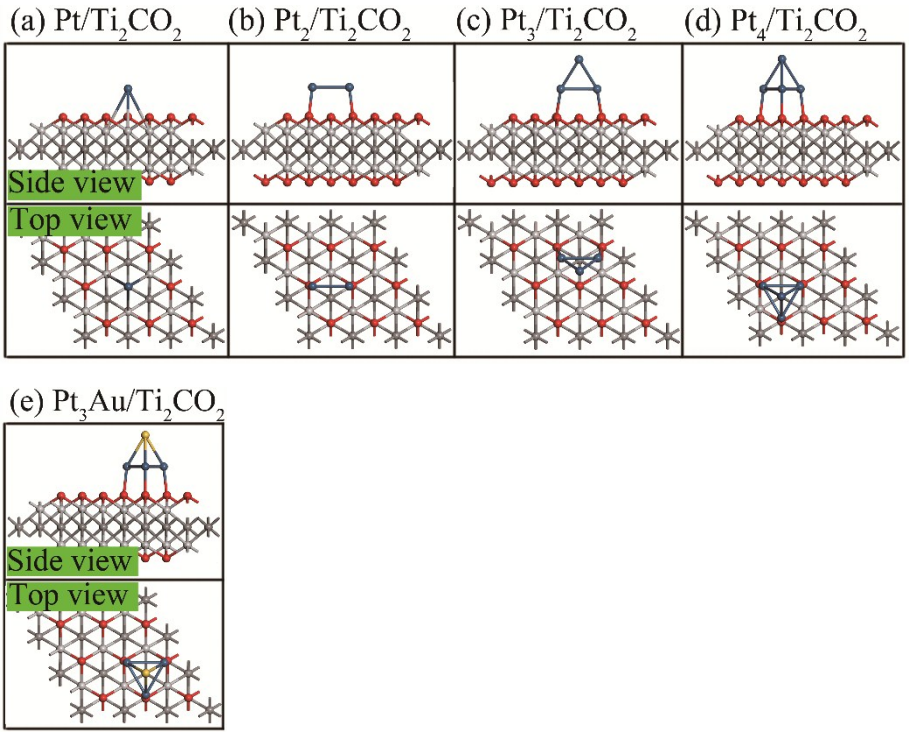

Fig. S6. Top and side views of the optimized geometric configurations of Pt/Ti_2CO_2, Pt_2/Ti_2CO_2, Pt_3/Ti_2CO_2, Pt_4/Ti_2CO_2 and Pt_3Au/Ti_2CO_2 systems.

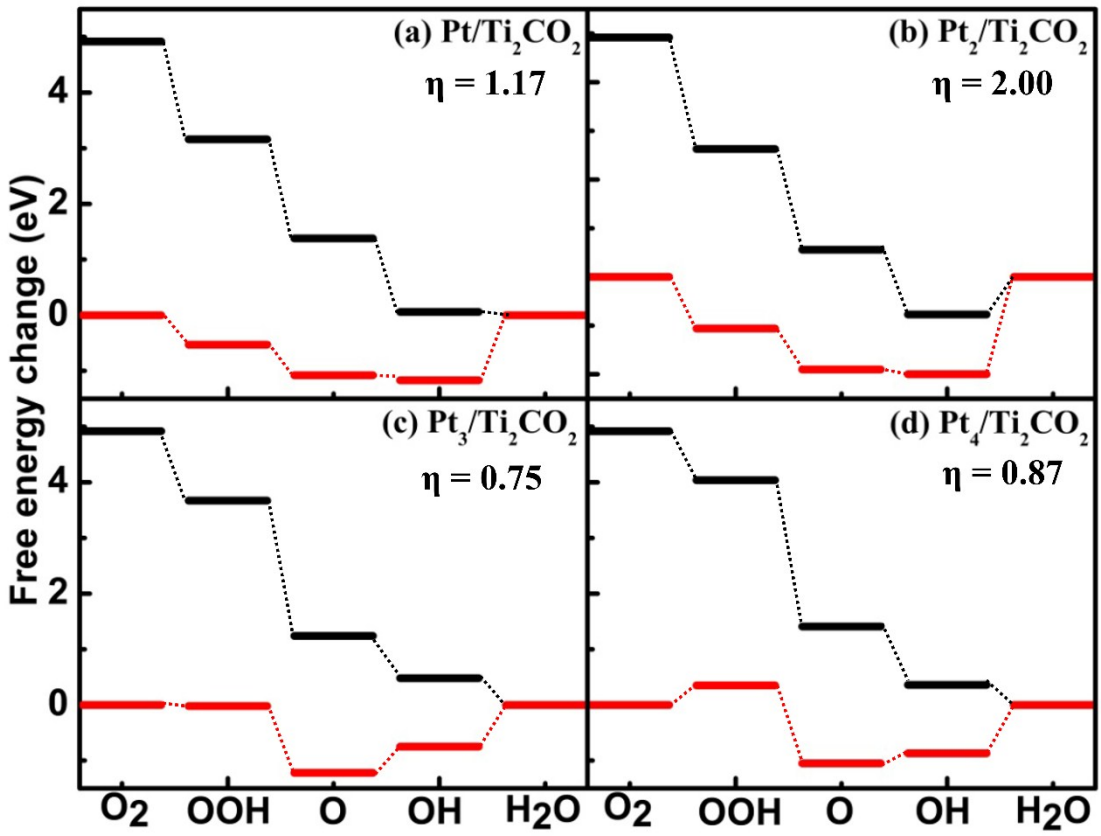

Fig. S7. The ORR free-energy diagrams on Pt/Ti_2CO_2, Pt_2/Ti_2CO_2, Pt_3/Ti_2CO_2, and Pt_4/Ti_2CO_2. The black and red lines are the free energy change of ORR at the zero potential and equilibrium potential, respectively.

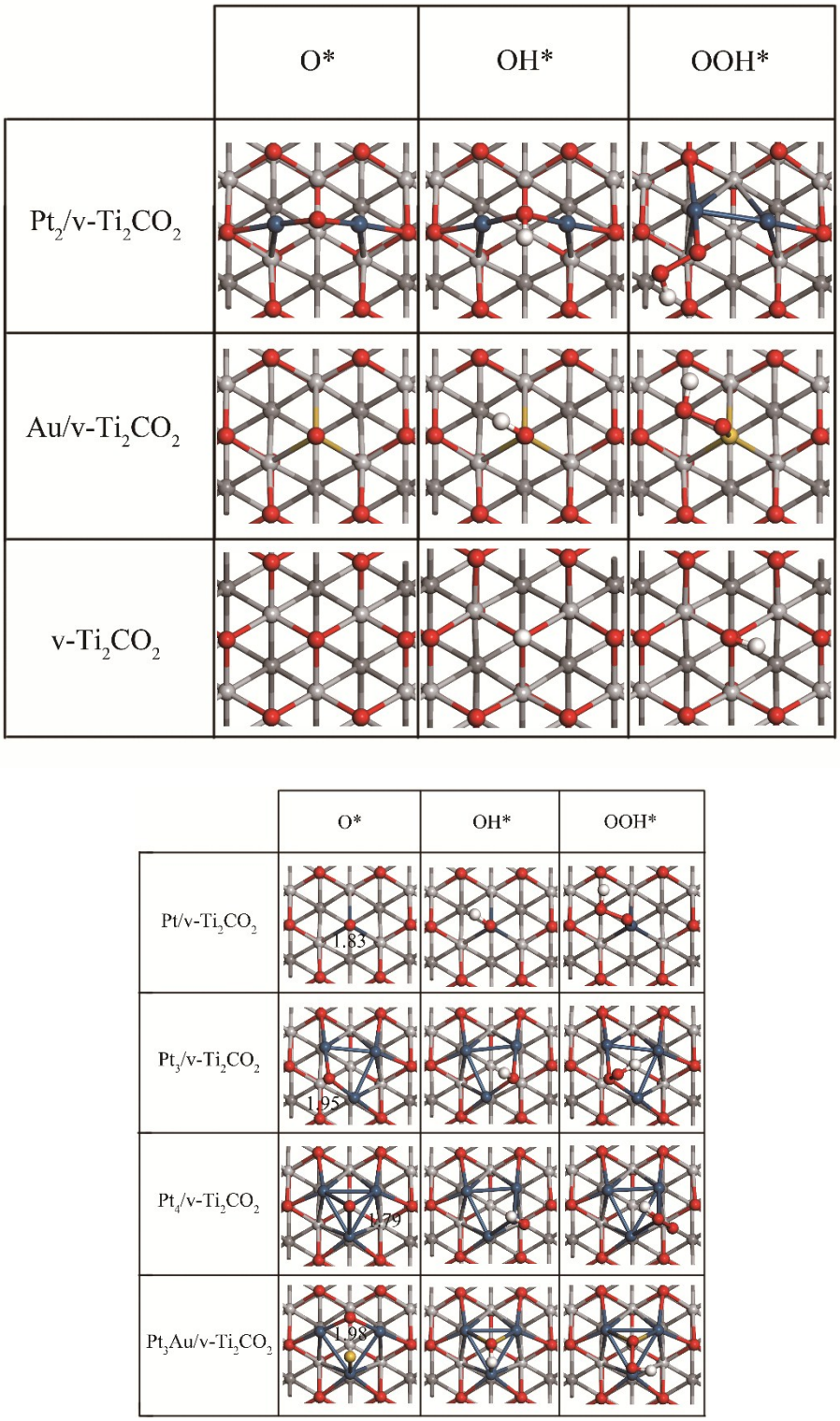

Fig. S8. The most stable geometric structures of the adsorbed O*, OH* and OOH* on the considered catalysts. The bonding is represented by '*'.

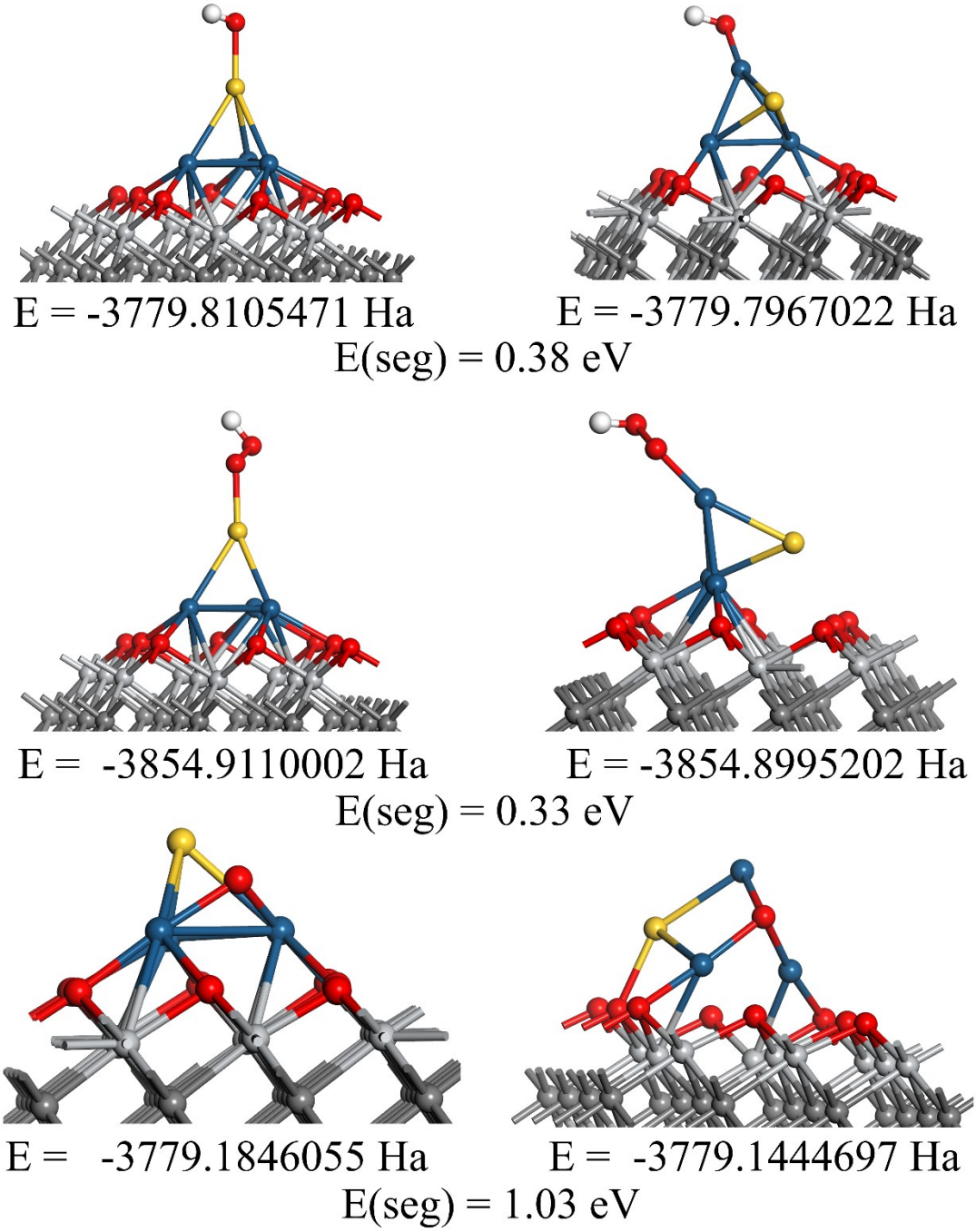

Fig. S9. The geometries, total energies, and segregation energies of Pt with the adsorption of O, OH, and OOH.

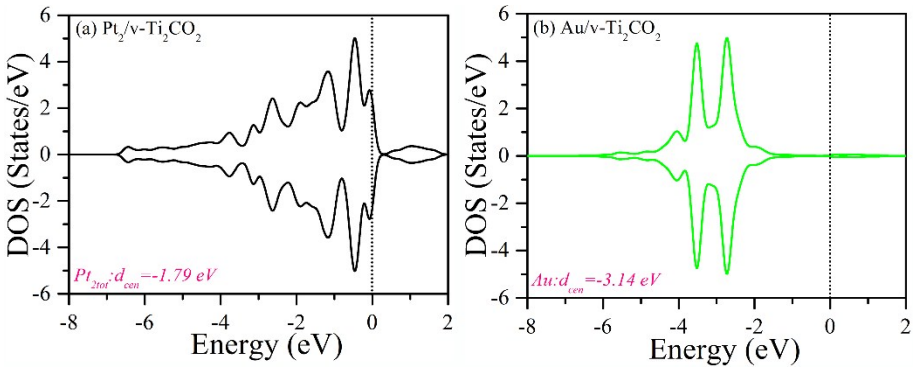

Fig. S10. The PDOSs of (a) Pt_2/v-Ti_2CO_2 and (b) Au/v-Ti_2CO_2. The positive and negative PDOSs represent the spin-up and spin-down channels, respectively. The d-band center (d_{cen}) of supported Pt atoms and Au atom connected to O is shown. The Pt_{2tot} (denoted by the black full line) represents the total PDOS of the Pt dimer in Pt_2/v-Ti_2CO_2. The Au (denoted by the green full line) represents the total PDOS of the single Au atom in Au/v-Ti_2CO_2. The Fermi level is denoted by a vertical dashed line.

As shown in the charge density difference (CDD) plots (Fig. S11), the accumulation of electrons (yellow region) mainly centers at the O atom and the depletion of electrons around the active sites connected with the O atom can be reflected by the blue region. The blue region between O and Pt are gradually apparent with the enhanced ORR activity of the catalysts, indicating the enhanced interaction around O and Pt, which is mainly due to the transferred electrons of the substrate.

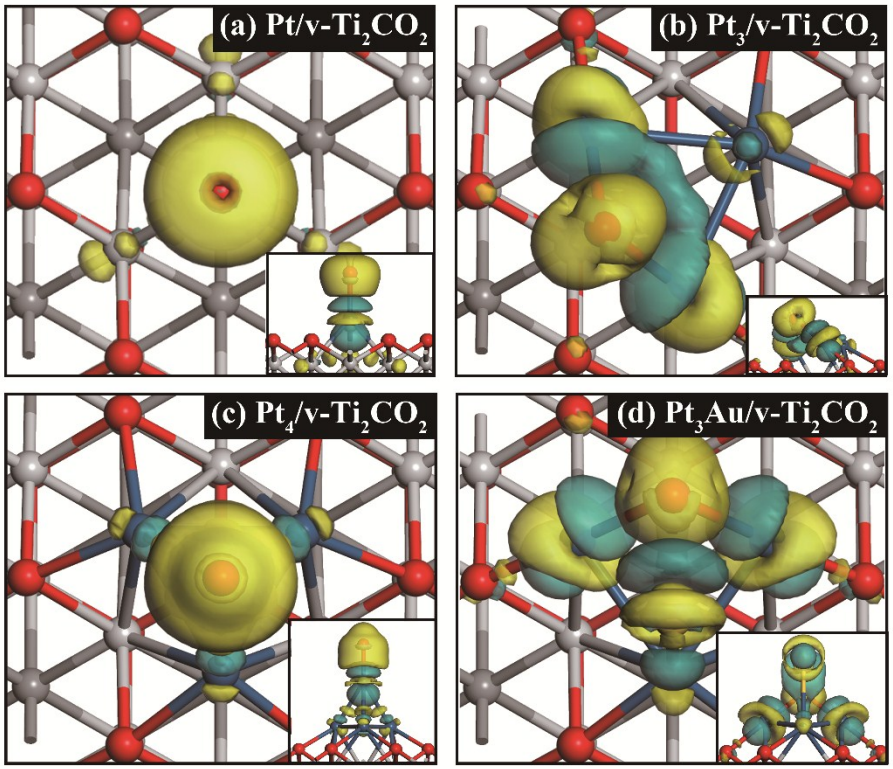

Fig. S11. The charge density difference (CDD) plots of adsorbed O* on different Pt-based surfaces. The yellow and blue region denotes the accumulation and depletion of electrons. The value of isosurfaces is set as ±0.02 e·Å^{-3}.

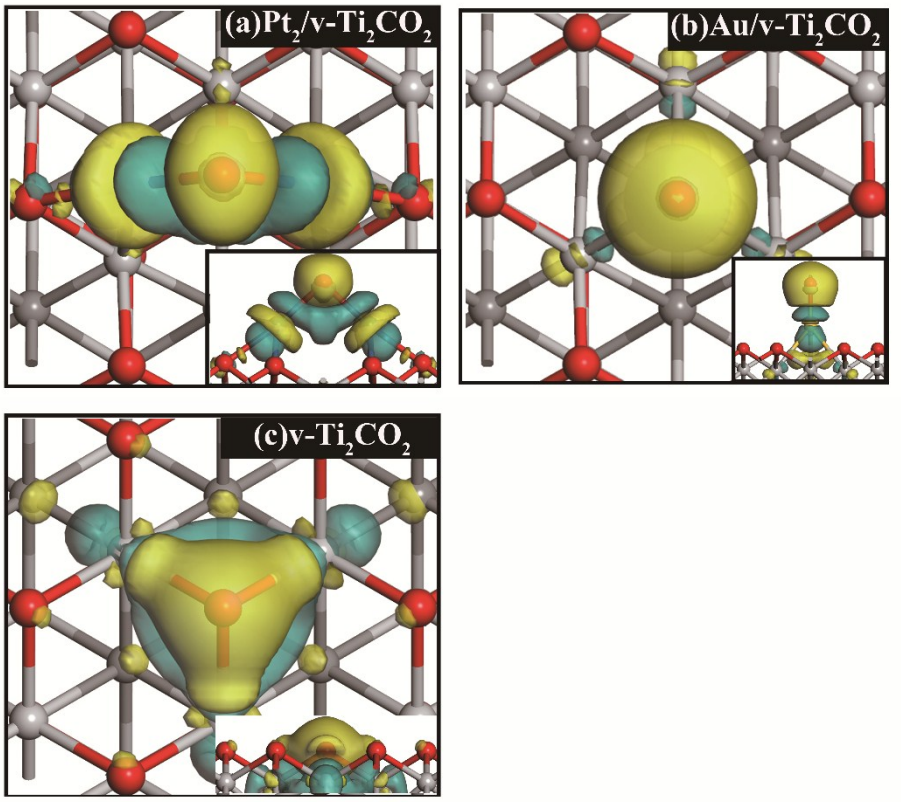

Figure. S12. The charge density difference (CDD) plots for adsorbed O* at the most stable configurations on Pt_2/v-Ti_2CO_2, Au/v-Ti_2CO_2 and v-Ti_2CO_2 with the isosurfaces of ±0.02 e·Å^{-3}. The yellow and blue region denotes the accumulation and depletion of electrons.

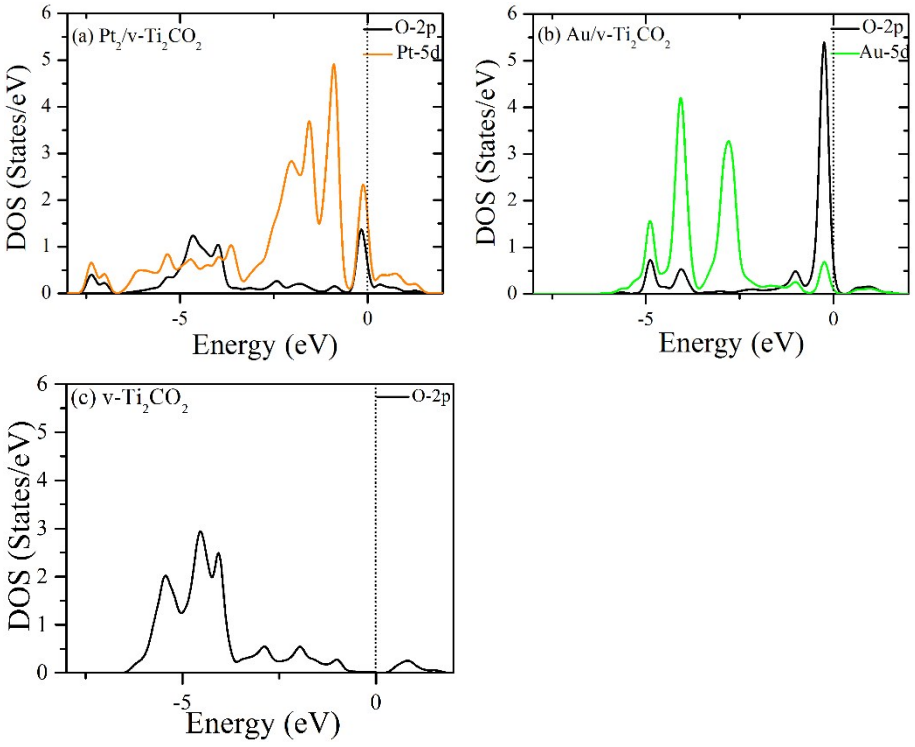

Fig. S13. The spin-up projected density of states (PDOSs) of adsorbed O species on the Pt_2/v-Ti_2CO_2, Au/v-Ti_2CO_2 and v-Ti_2CO_2, respectively. The Fermi energy level is represented by the vertical dotted line.

Table S1. The zero point energies (ZPE) and entropic corrections (TS) of oxygenates at T = 298.15 K (in eV). The values of H_2 and H_2O molecules are taken from the NIST data base. The values of O*, OH* and OOH* are obtained based on the vibrational frequencies. Constant values of ZPE and TS are used for each oxygenated intermediates of catalytic surfaces in the present work.

Species	ZPE [1]	TS [1]	ZPE [2]	TS [2]	ZPE [3]	TS [3]
O*	0.08	-0.01	0.10	0.13	0.09	-0.03
OH*	0.39	0.03	0.40	0.13	0.40	-0.05
OOH*	0.46	0.07	0.53	0.26	0.45	-0.15
O_2	--	--	--	--	--	--
H_2	0.27	0.41	0.27	0.41	0.27	0.41
H_2O	0.56	0.67	0.56	0.67	0.56	0.67

[1] Zhou S, Yang X, Pei W, Liu N, Zhao J. Heterostructures of MXenes and N-doped graphene as highly active bifunctional electrocatalysts[J]. *Nanoscale*, 2018, 10: 10876-10883.

[2] Liu CY, Li EY. Termination Effects of Pt/v-Ti n+1C nT2 MXene Surfaces for Oxygen Reduction Reaction Catalysis[J]. *ACS Appl Mater Interfaces*, 2019, 11: 1638-1644.

[3] The present work.

Table S2. Mulliken charge analysis for different surfaces of Pt_n/v-Ti_2CO_2 (n = 1-4), Pt_3Au/v-Ti_2CO_2 and Au/v-Ti_2CO_2 (q (s), in |e|). The positive and negative value illustrates the donation and accumulation of electrons, respectively.

	q (Pt1)	q (Pt2)	q (Pt3)	q (Pt4)	q (Au)
Pt/v-Ti_2CO_2	-0.36	--	--	--	--
Pt_2/v-Ti_2CO_2	-0.30	-0.30	--	--	--
Pt_3/v-Ti_2CO_2	-0.21	-0.20	-0.21	--	--
Pt_4/v-Ti_2CO_2	-0.13	-0.15	-0.16	-0.09	--
Pt_3Au/v-Ti_2CO_2	-0.19	-0.19	-0.19	--	0.08
Au/v-Ti_2CO_2	--	--	--	--	-0.21

Table S3. The adsorption free energy (ΔG, in eV) of O*, OH* and OOH* on the Pt_2/v-Ti_2CO_2, Au/v-Ti_2CO_2 and v-Ti_2CO_2. The most stable adsorption sites of the intermediate are shown in the brackets.

Species	Pt_2/v-Ti_2CO_2	Au/v-Ti_2CO_2	v-Ti_2CO_2
ΔG_{O*}	1.18 (bri)	4.01 (top)	-1.47 (hollow)
ΔG_{OH*}	0.28 (bri)	1.58 (top)	-1.65 (hollow)
ΔG_{OOH*}	3.63 (top)	4.77 (top)	2.04 (hollow)

Table S4. Mulliken charge analysis of the adsorbed O* intermediates on Pt_2/v-Ti_2CO_2, Au/v-Ti_2CO_2 and the v-Ti_2CO_2 surfaces (q (s), in |e|). The positive and negative net charge value illustrates the donation and accumulation of electrons, respectively.

	q (O)	q (Pt1)	q (Pt2)	q (Au)
Pt_2/v-Ti_2CO_2	-0.69	0.40	0.40	--
Au/v-Ti_2CO_2	-0.63	--	--	0.14
v-Ti_2CO_2	-0.89	--	--	--

Table S5. Mulliken charge analysis of the adsorbed OH* intermediates on the Pt_n/v-Ti_2CO_2 (n = 1-4), Pt_3Au/v-Ti_2CO_2, Au/v-Ti_2CO_2 and the v-Ti_2CO_2 surfaces (q (s), in |e|).The positive and negative net charge value illustrates the donation and accumulation of electrons, respectively.

	q (OH)	q (Pt1)	q (Pt2)	q (Pt3)	q (Pt4)	q (Au)
Pt/v-Ti_2CO_2	-0.34	0.09	--	--	--	--
Pt_2/v-Ti_2CO_2	-0.28	0.28	0.28	--	--	--
Pt_3/v-Ti_2CO_2	-0.19	0.05	0.24	0.26	--	--
Pt_4/v-Ti_2CO_2	-0.31	0.01	-0.06	-0.06	0.10	--
Pt_3Au/v-Ti_2CO_2	-0.34	0.01	0.02	0.01	--	0
Au/v-Ti_2CO_2	-0.38	--	--	--	--	0.05
v-Ti_2CO_2	-0.48	--	--	--	--	--

Table S6. Mulliken charge analysis of the adsorbed OOH* intermediates on the Pt_n/v-Ti_2CO_2 (n = 1-4), Pt_3Au/v-Ti_2CO_2, Au/v-Ti_2CO_2 and the v-Ti_2CO_2 surfaces (q (s), in |e|).The positive and negative net charge value illustrates the donation and accumulation of electrons, respectively.

	q (OOH)	q (Pt1)	q (Pt2)	q (Pt3)	q (Pt4)	q (Au)
Pt/v-Ti_2CO_2	-0.21	0.07	--	--	--	--
Pt_2/v-Ti_2CO_2	-0.26	0.30	0.09	--	--	--
Pt_3/v-Ti_2CO_2	-0.26	0.29	0.28	0.02	--	--
Pt_4/v-Ti_2CO_2	-0.26	0.00	-0.07	-0.07	0.09	--
Pt_3Au/v-Ti_2CO_2	-0.30	0.00	0.02	0.00	--	0.03
Au/v-Ti_2CO_2	-0.26	--	--	--	--	0.05
v-Ti_2CO_2	-0.57	--	--	--	--	--